

# Simulation of reach-scale water and heat fluxes across the river-groundwater interface for retrieving hyporheic residence times and temperature dynamics

Matthias Munz<sup>1</sup>, Sascha Oswald<sup>1</sup> and Christian Schmidt<sup>2</sup>

<sup>1</sup>University of Potsdam, Institute of Earth and Environmental Science, Karl-Liebknecht-Str. 24-25, 14476 Potsdam

<sup>2</sup>Helmholtz-Centre for Environmental Research - UFZ, Permoserstraße 15, 04318 Leipzig, Germany

## 1. Introduction

Flow patterns in conjunction with seasonal and diurnal temperature variations control ecological and biogeochemical conditions in hyporheic sediments. In particular, hyporheic temperatures have a great impact on many temperature-sensitive microbial processes. In this study, we used 3D coupled water flow and heat transport simulations applying the HydroGeoSphere code in combination with high resolution observations of hydraulic heads and temperatures to quantify reach-scale water and heat flux across the river-groundwater interface and hyporheic temperature dynamics of a lowland gravel-bed river. Based on the simulation results we derived a general empirical relationship, estimating the influence of hyporheic flow path residence time on hyporheic flow path temperature. Furthermore we used an empirical temperature relationship between effective temperature and respiration rate to estimate the influence of hyporheic flow path residence time and temperature on hyporheic oxygen consumption. This study highlights the relation between complex hyporheic temperature patterns, hyporheic residence times and their implications on temperature sensitive biogeochemical processes.

## 2. Study side and data collection

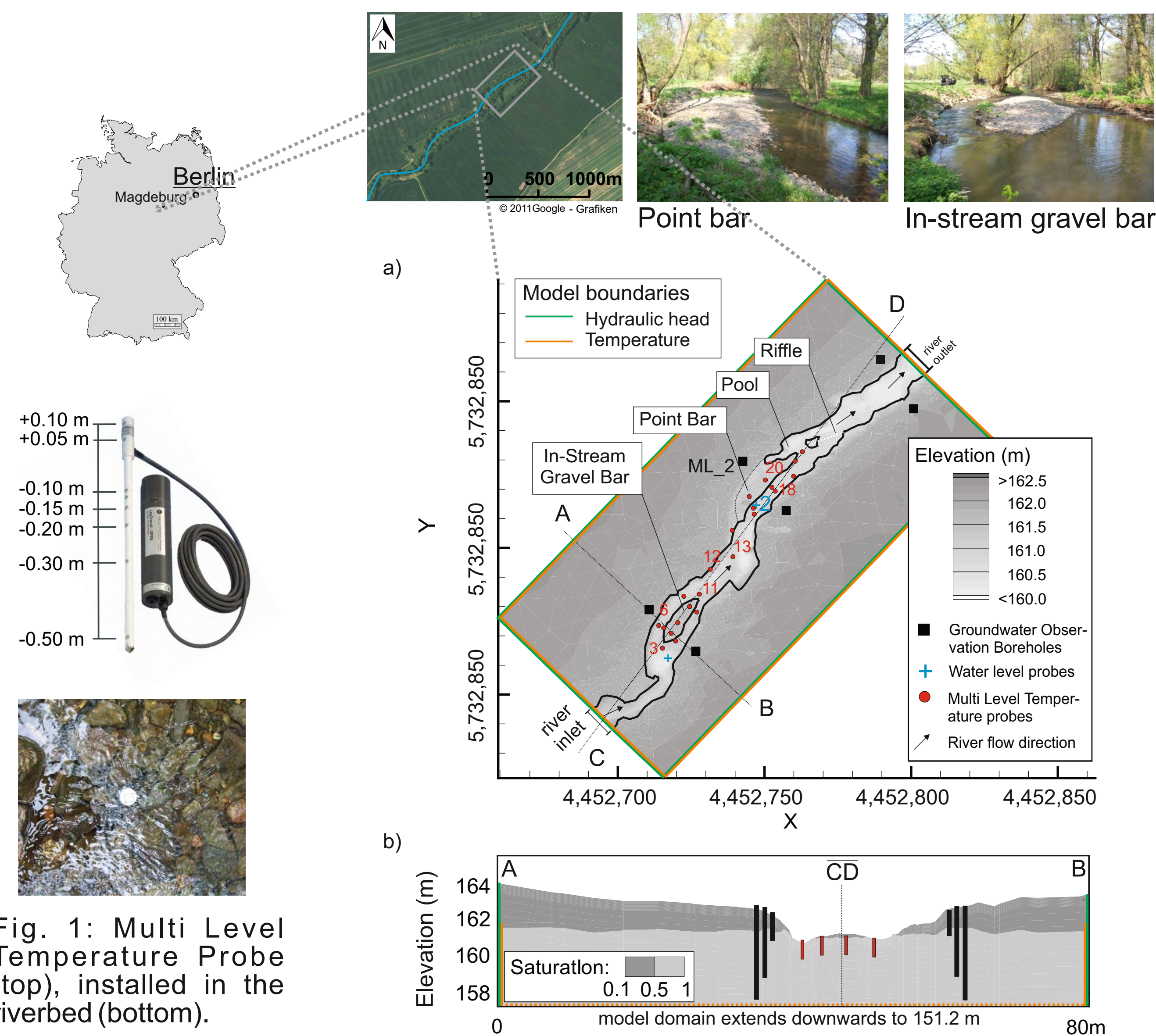


Fig. 1: Multi Level Temperature Probe (top), installed in the riverbed (bottom).

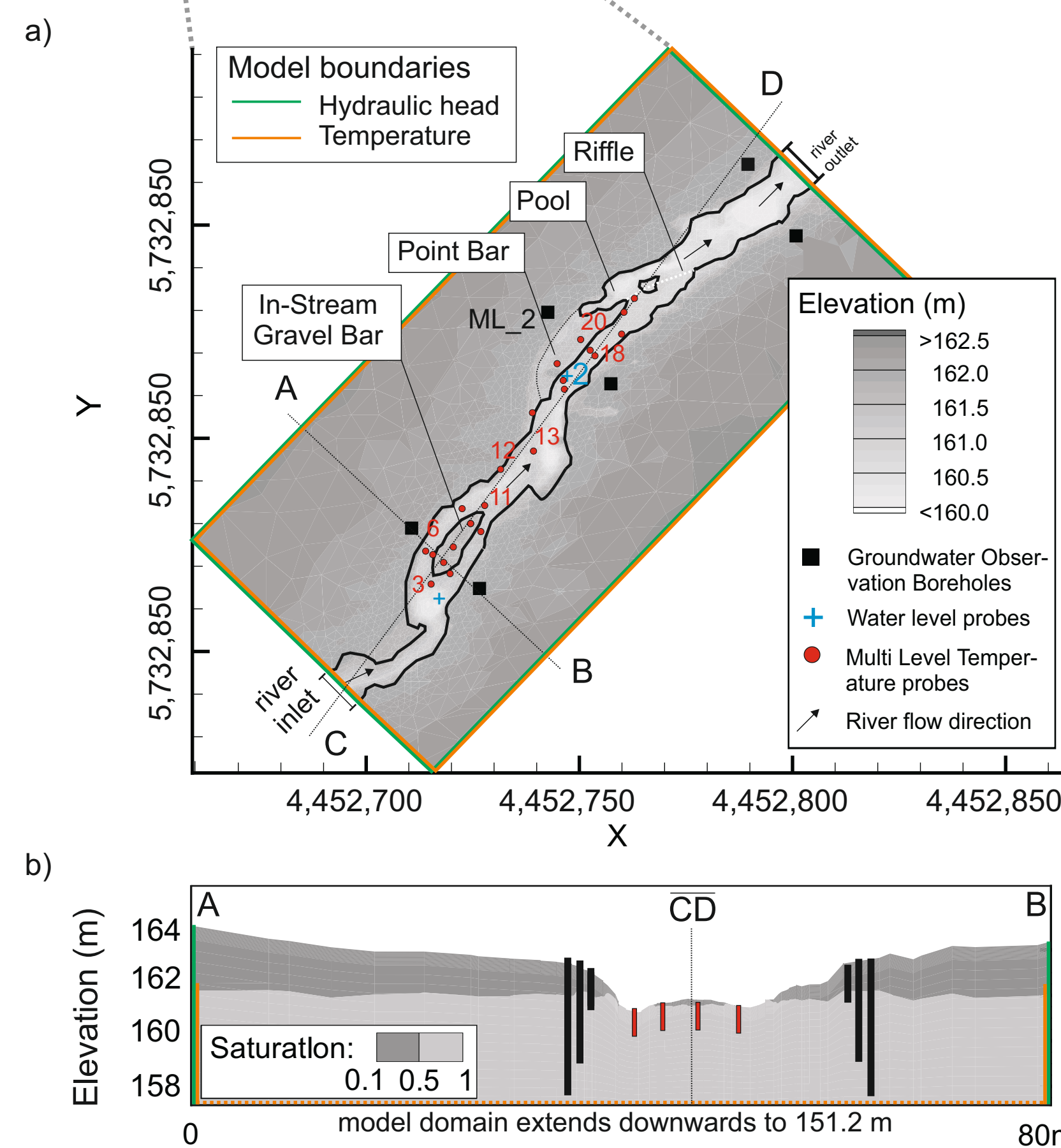


Fig. 2: (a) Study site and model domain, showing the experimental infrastructure, surface elevation, relevant geomorphological structures, and the finite element mesh (white-framed triangles). The black line indicates the river shape for discharges, here taken of  $0.25 \text{ m}^3 \text{ s}^{-1}$ . (b) Cross-section through the model domain (A to B). The lower 6 metres of the model domain are not shown, because they are fully saturated and no observation boreholes extended to that depth.

## 3. HydroGeoSphere model setup

### Discretisation

The dimensions of the model domain were  $80 \text{ m} \times 160 \text{ m} \times 13 \text{ m}$  (width, length, thickness; Fig. 2). Element size was set to 10 m in the floodplain, but subsequently refined to 0.25 m in the riverbed.

### Boundary condition

- Prescribed hydraulic head and groundwater temperature at the sides of the model domain
- Prescribed water flux and river temperature at the river inlet
- Critical-depth boundary is applied at the river outlet
- Atmospheric energy input calculated by means of the ambient air temperature and incoming short and long wave solar radiation

### Parameterisation

Hydraulic conductivity ( $K_h$ ) was generated by Sequential Gaussian Simulation (mean =  $8.3 \times 10^{-4} \text{ m s}^{-1}$ , var =  $5.1 \times 10^{-7} \text{ m}^2 \text{ s}^{-2}$ , range = 25 m); estimation based on slug test measurements along the river reach. Parameters classified as sensitive to the simulation results ( $K_h$ -mean,  $K_h$ -var,  $K_h$ -range,  $K_h$ -anisotropy, riverbed roughness, heat capacity and thermal conductivity of the solids) were calibrated using PEST for a 90-day period from Oct. 2011 to Jan. 2012.

## 4. Model validation

The magnitude and variations of the simulated temperatures matched the observed ones, with an average mean absolute error of  $0.7 \text{ }^\circ\text{C}$  and an average Nash Sutcliffe Efficiency of 0.87.

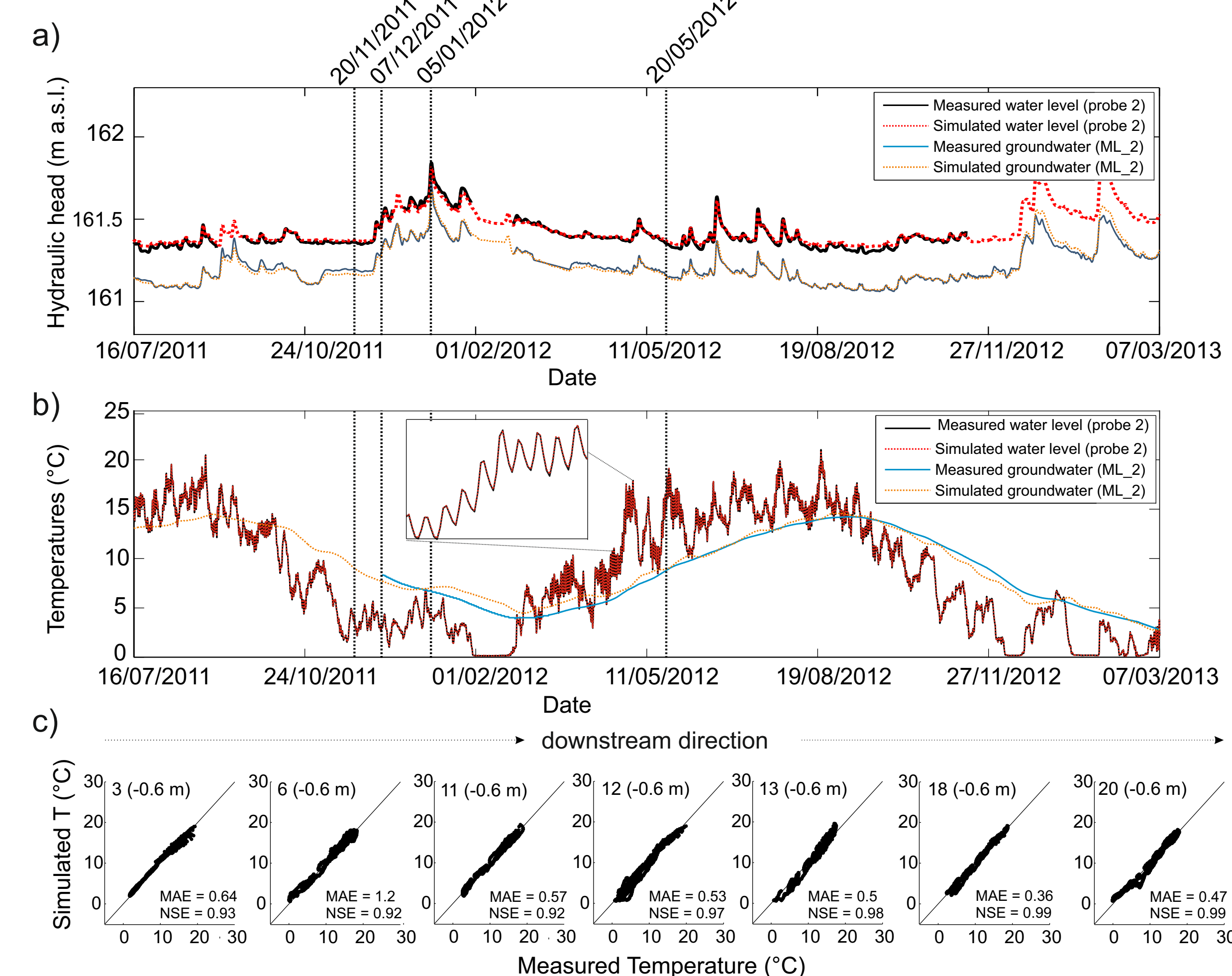


Fig. 3: (a) Observed and simulated hydraulic heads, (b) observed and simulated temperatures and (c) measured vs. simulated riverbed temperatures of the calibrated model. All measurement locations are indicated in Fig. 2 a.

## 4. Subsurface flow field and temperature patterns

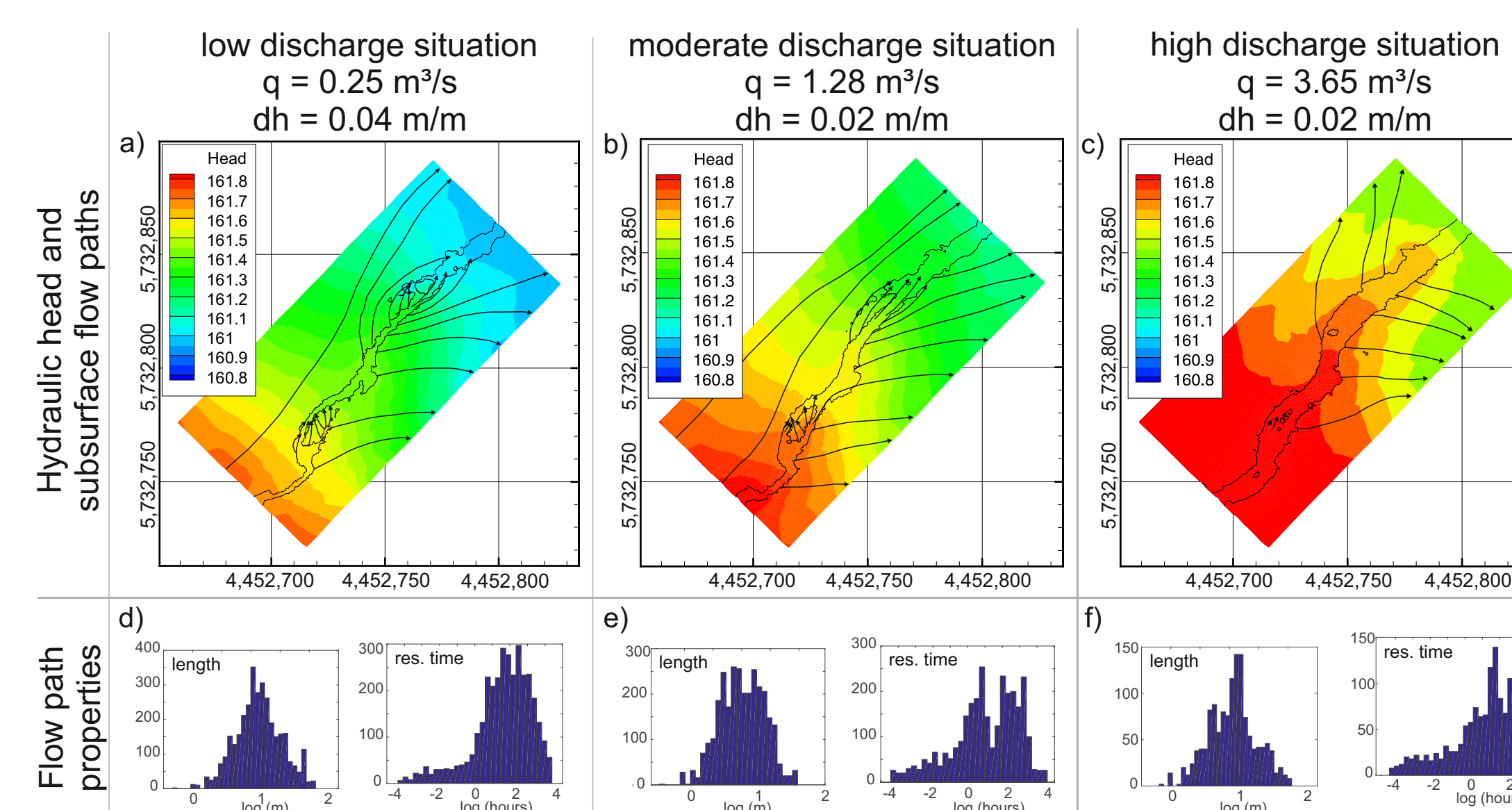


Fig. 4: (a-c) Hydraulic heads of the streambed and groundwater streamlines for low, moderate and high river discharges under losing conditions. (d-f) Flow path length and residence time distributions for hyporheic flow path.

Cross-sections along transect A-B (Fig.2):

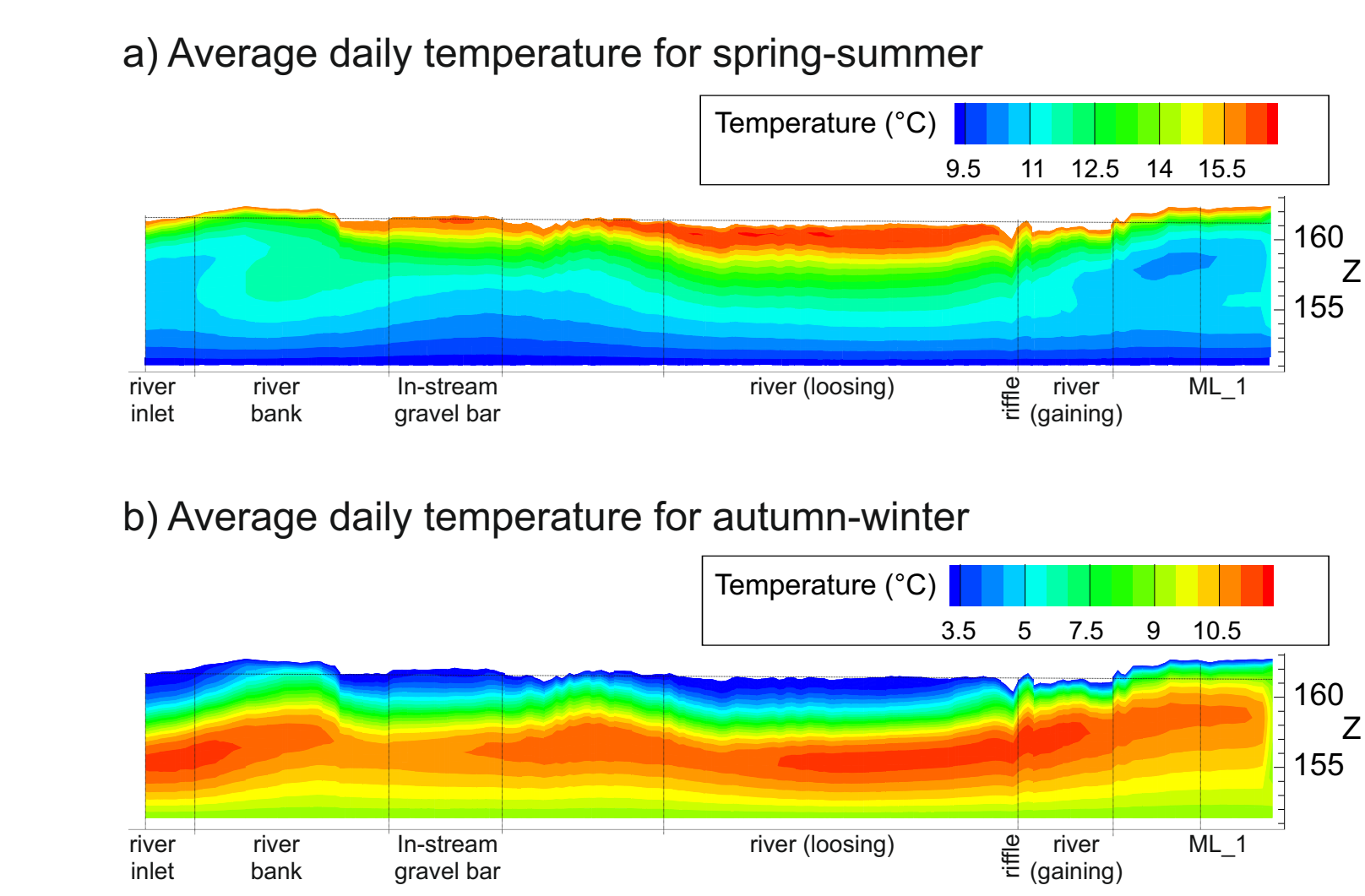


Fig. 5: (a) Daily average temperatures for spring-summer, (b) autumn-winter.

## 5. Implications of hyporheic residence time and temperature for biogeochemical processes in the streambed

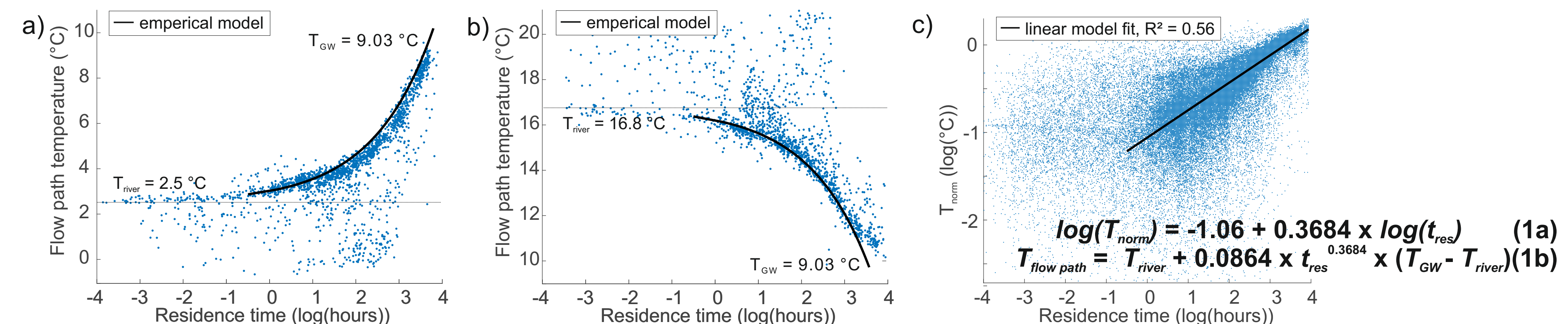


Fig. 6: Relation between residence time of hyporheic flow paths ( $t_{res}$ ) versus average flow path temperature ( $T_{flowpath}$ ) for (a) an autumn day (22 November 2011) and (b) a spring day (20 May 2012). The empirical model is presented in equation 1b. (c) Relation between residence time of hyporheic flow paths versus normalized flow path temperature ( $T_{norm}$ ) for all simulation time steps, with temperature differences between river ( $T_{river}$ ) and groundwater ( $T_{gw}$ )  $> 3 \text{ }^\circ\text{C}$ . The fitted linear model is presented in equation 1a.

## 6. Summary and conclusions

The calibrated and validated 3D fully-integrated model of reach-scale water and heat fluxes across the river-groundwater interface was able to accurately represent the real system. The simulation results showed that non submerged streambed structures caused significant thermal heterogeneity within the saturated sediment at the reach scale. The average hyporheic flow path temperature was found to strongly correlate with the flow path residence time (flow path length) and the temperature gradient between river and groundwater. Despite the complexity of these processes, the simulation results allowed the derivation of a general empirical relationship between the hyporheic residence times and temperature patterns (eq. 1). Based on this empirical relation we furthermore quantified the influence of hyporheic flow path residence time and temperature on oxygen consumption (Fig. 7).

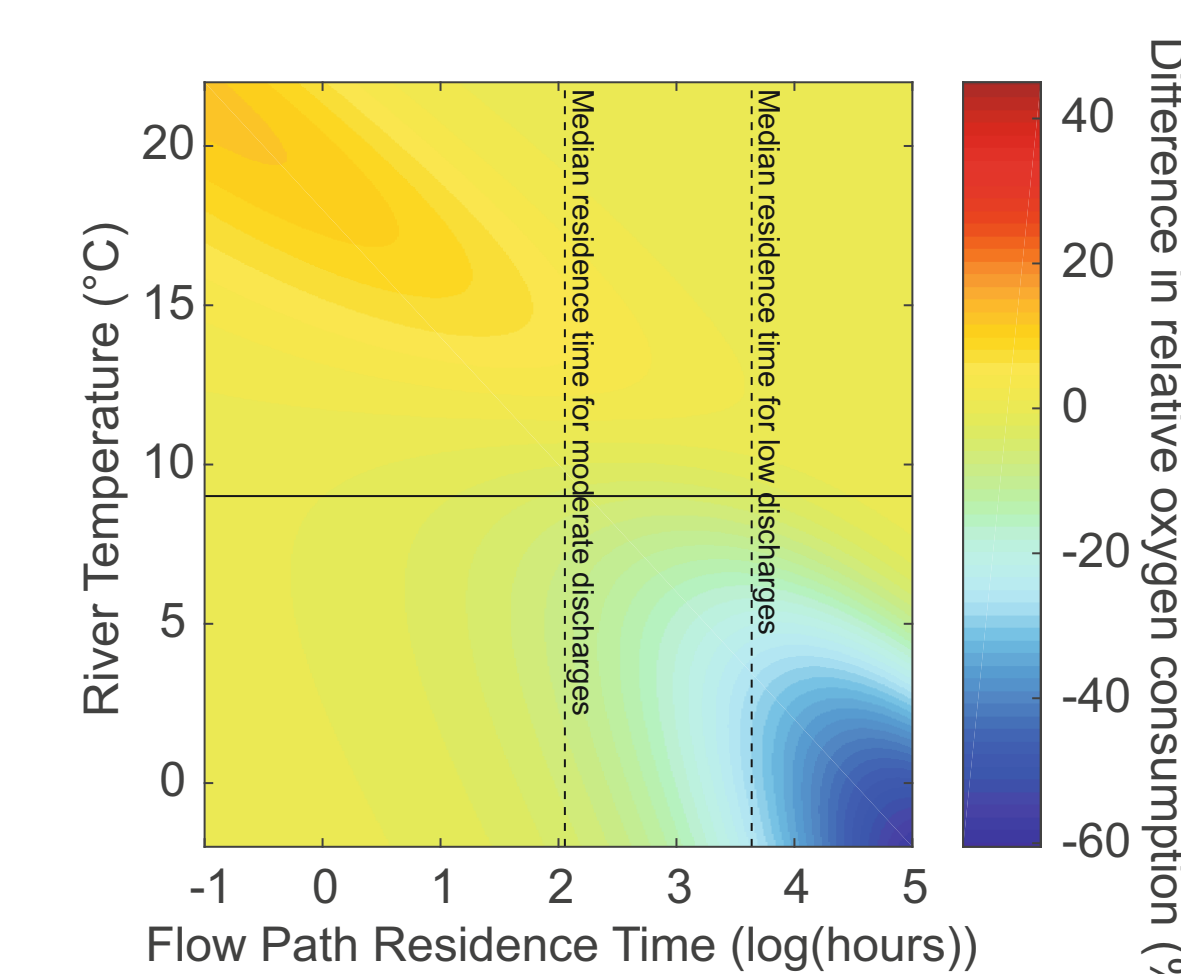


Fig. 7: Difference between empirical oxygen consumption calculated via river temperature and via empirical flow path temperature (Equation 1b).